Journal of Hazardous Materials 166 (2009) 904–910

Contents lists available at ScienceDirect

Journal of Hazardous Materials

journal homepage: www.elsevier.com/locate/jhazmat

Rapid decolorization of azo dye methyl orange in aqueous solution by nanoscale zerovalent iron particles

Jing Fan [a,*], Yanhui Guo [a], Jianji Wang [a], Maohong Fan [b]

[a] School of Chemical and Environmental Sciences, Henan Key Laboratory for Environmental Pollution Control, Key Laboratory for Yellow and Huai River Water Environmental and Pollution Control, Ministry of Education, Henan Normal University, Xinxiang, Henan 453007, PR China
[b] School of Civil and Environmental Engineering, Georgia Institute of Technology, Atlanta, GA 30332, USA

ARTICLE INFO

Article history:
Received 14 August 2008
Received in revised form 8 November 2008
Accepted 26 November 2008
Available online 3 December 2008

Keywords:
Nanoscale zerovalent iron
Azo dye
Decolorization
Methyl orange

ABSTRACT

Azo dyes are recalcitrant and refractory pollutants that constitute a significant burden on the environment. The report here is focused on the decolorization treatment of water soluble azo dye methyl orange (MO) by chemically synthesized nanoscale zerovalent iron (NZVI) particles. Experimental variables such as initial dye concentration, iron dosage, solution pH and temperature were studied systematically. Batch experiments suggest that the decolorization efficiency was enhanced with the increase of NZVI dosage and reaction temperature, but decreased with increasing initial dye concentration and initial solution pH. Further studies indicated that existence of inorganic salt (Na_2SO_4) could inhibit the decolorization of MO. Kinetic analyses based on the experimental data elucidated that the decolorization process followed a first order exponential decay kinetics model. The activation energy was determined to be 35.9 kJ/mol.

1. Introduction

Modern dyes have a multiple variety and they are often intended to be produced to resist the breakdown of long-term exposure to sunlight, water, and other atrocious conditions, thus making the treatment of dye wastewater more difficult. Within the overall category of synthetic textile dyestuffs, azo dyes constitute about a half of global production (700,000 ton per year), and during dyeing operation processes, about 15% of them ends up in wastewaters [1]. Decolorization treatment of azo dye effluents has therefore received increasing attention. Traditional physical and/or chemical methods such as flocculation and adsorption, simply transfer the pollutants to another phase rather than destroying them [2]. Some advanced oxidation processes (AOPs) have been used to mineralize dye molecules on the basis of the generation of hydroxyl radicals (•OH) in water. They are technically viable clean-up processes for dyes, but have some limits. For example, homogeneous Fenton and photo-assisted Fenton reaction process have tight working pH range (pH 2–4) and they may generate large volumes of iron sludge for further disposal [3]. Heterogeneous photo-catalytic degradation using titanium dioxide has been widely studied in laboratory. However, it is not desirable for a practical remediation technology due to the serious problems like low quantum yields caused by hole-electron recombination and the requirement of UV light [4,5]. Moreover, all these methods are insufficient to treat azo dye wastewater with high concentration and high chroma [6]. Because azo dyes are especially resistant in the natural environment, their biological degradation has serious obstacles [7]. Therefore, the preferred techniques for the treatment of azo dye wastewater should be based on the combination of pre-treatment and biological methods, and an effective pre-treatment process can enhance significantly the biodegradability of the azo dyes. Zerovalent iron (ZVI), an environmentally friendly reducing agent, can reduce the azo bond, cleaving dye molecules into products that are more amenable to mineralization in biological treatment processes [8]. Much attention has been paid on the treatment of azo dyes by ZVI in recent years [9–12]. The advantages of the ZVI decolorization process include the ease in use as a pre-treatment process, easy recycling of the spent iron powder by magnetism as well as low iron concentration remaining and no necessity for further treatment of the effluents [11]. However, traditional ZVI methods to date almost used commercial grade zerovalent iron which has relatively low reactivity, and needs prolonged reaction time and low pH condition for adequate treatment. These disadvantages can be overcome by increasing the activity of Fe^0 particles through decreasing their sizes to nanoscale. Due to the smaller particle size, larger specific surface area, higher density of reactive surface sites and greater intrinsic reactivity of surface sites [13], nanoscale zerovalent iron (NZVI) has gained prominence for environmental remediation, especially for the remediation of contaminants that are susceptible to reductive transformation such as halogenated

* Corresponding author. Tel.: +86 373 3325971; fax: +86 373 3326445.
E-mail address: fanjing@henannu.edu.cn (J. Fan).

0304-3894/$ – see front matter © 2008 Elsevier B.V. All rights reserved.
doi:10.1016/j.jhazmat.2008.11.091

organics [14–17], high valent heavy metals [18–20], and toxic inorganic anions [21–23]. Nevertheless, very few information on the decolorization of azo dye by NZVI is available in literature [5,24].

Methyl orange (MO) is a model compound of a series of common water soluble azo dyes widely used in chemistry, textiles and paper industries. In the present work, the decolorization efficiency of MO by self-synthesized NZVI particles was evaluated by studying the effects of experimental variables such as initial MO concentration, NZVI dosage, solution pH, temperature, and inorganic salt (Na_2SO_4). The degradation products and reaction kinetics for the decolorization process were also investigated in some details.

2. Experimental

2.1. Materials

Sodium borohydride was purchased from Sinopharm Chemical Reagent Co. (Shanghai,China). Ferric chloride ($FeCl_3{\cdot}6H_2O$) was obtained from Tianjin Chemical Reagent Co. (Tianjin, China). Methyl range ($C_{14}H_{14}N_3SO_3Na$, C.I.13025) was from Beijing Chemical Reagent Co. (Beijing, China). All other reagents were analytical reagent grade. Deionized water was used throughout this study.

2.2. Preparation of NZVI particles

NZVI particles were prepared by liquid phase reduction method [25]. All solvents were degassed and saturated with N_2 before use. 1.6 M aqueous $NaBH_4$ solution was added drop-wise into equal volume of 1.0 M solution of $FeCl_3{\cdot}6H_2O$ during vigorously stirring under N_2 atmosphere. The reaction can be described by the equation [26]:

$$4Fe^{3+} + 3BH_4^- + 9H_2O \rightarrow 4Fe^0 + 3H_2BO_3^- + 12H^+ + 6H_2 \quad (1)$$

After the reaction, the solution was kept stirring for another 20 min. Then the solid was vacuum-filtered and washed with degassed dilute hydrochloric acid, deionized water and 1:1 (v/v) ethanol/acetone. The resulting gray–black solid was vacuum-dried.

2.3. Characterization of the synthesized NZVI particles

The morphology and size of the particles were observed with a JEM 100CX-II transmission electron microscopy (TEM, JEM Company, Japan). Samples for TEM analysis were prepared by dispersing the particles in ethanol using ultrasonic agitation. A drop of the suspension was placed on a copper TEM grid and allowed to evaporate.

The crystal structure of the final product was examined by a Bluker D8-Advance X-ray diffractometer (XRD, Germany) with Cu Kα radiation. The operating voltage was set at 40 kV, and the current was 40 mA.

2.4. Decolorization procedures

The stock solution was prepared with appropriate amount of MO in 1 L deionized water. Batch experiments were carried out in a glass flask with a flat bottom. The reaction of MO with NZVI was investigated at different factors, including the initial MO concentration, the NZVI dosage, the initial solution pH, reaction temperature, and coexistent inorganic salt Na_2SO_4. The desired initial pH value of MO solution was adjusted by diluted HCl or NaOH and determined by a digital pH meter (pHS-3C, Shanghai, China). In a typical experiment, MO solution with a known concentration was purged with N_2 for 20 min at a given temperature in a water bath. After adding a desired amount of NZVI particles, the solution was ultrasonically dispersed for 1 min in an ultrasonic cleaning bath (KQ3200DB, Kunshan, China). Then the flask was immediately put into a thermostatically controlled shaker (TSHZ-A, Shanghai, China) working at 120 rpm. At preset time intervals, samples were taken by a glass syringe and filtered through 0.45 μm membrane filter.

2.5. Analytical methods

The UV–vis spectra of MO were recorded from 200 to 750 nm using a UV–vis spectrophotometer (TU1900-PC, Beijing, China) equipped with a quartz cell of 1.0 cm path length. The concentrations of MO samples were quantified by measuring the absorption intensity at λ_{max} = 465 nm. If needed, sample solution was diluted five times before measurement. The decolorization efficiency of MO was defined as follows:

$$\text{decolorization efficiency} = \left(1 - \frac{C_t}{C_0}\right) \times 100\% \quad (2)$$

where C_0 is the initial concentration of MO, and C_t is the concentration of MO at reaction time t (min).

When the decolorization reaction completed, 80 ml of the solution was filtrated and concentrated in a rotary evaporator, then the residue was dissolved by 40 ml ethanol. The sample was analyzed employing a gas chromatography–mass spectrometry (6890/5793N GC–MS, Agillent Corporation, USA). A HP-5 capillary column (30 m × 0.25 mm × 0.25 μm; Hewlett Packard, USA,) was used. The column temperature was held at 50 °C for 2 min and was then increased from 50 to 240 °C at a rate of 10 °C per min.

3. Results and discussion

3.1. Characterization of the NZVI particles

Fig. 1 shows the image of the synthesized NZVI particles observed by TEM. The particles prepared in this work have a nearly spherical shape with a grain size range about 20–80 nm. Fig. 1(a) and (b) was obtained from different regions on the copper TEM grid with a magnification of 20,000. It is a common behavior that

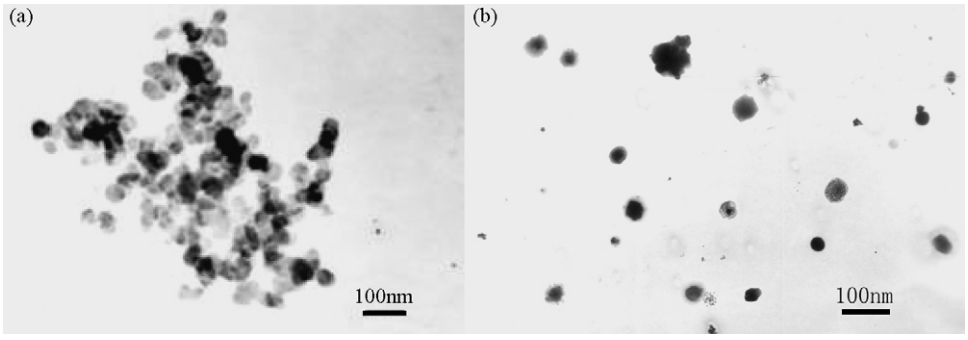

Fig. 1. TEM image of NZVI particles with a magnification of 20,000: (a) aggregates of iron particles; (b) single iron particles.

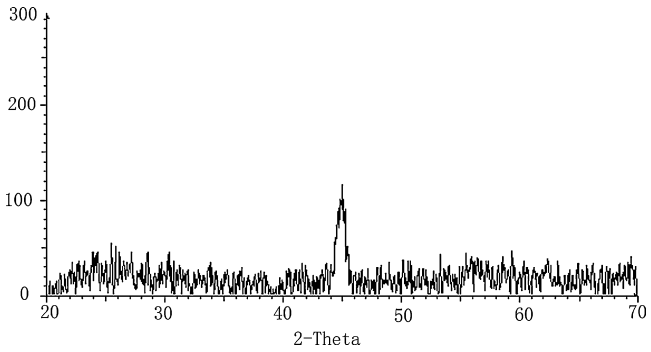

Fig. 2. XRD pattern of NZVI particles: Cu Kα radiation; operating voltage 40 kV; current 40 mA.

nanoparticles would easily aggregate because of the magnetic property of nanoparticles themselves, so most of the particles exist in chain-like aggregates (Fig. 1(a)). A few single particles showed in Fig. 1(b) may come from the dispersing effect of ultrasonic agitation.

XRD pattern of dry NZVI particles was shown in Fig. 2. The apparent peak at the 2θ of 44.86° indicated the presence of zerovalent iron. The broad iron peak implied that the synthesized NZVI particles possess a chemically disordered crystal structure.

3.2. Decolorization reaction mechanism analysis

The role of NZVI particles in the decolorization reaction process is suggested as follows: (i) strong reductive and catalysis, (ii) micro-electrolysis, and (iii) adsorption and flocculation. NZVI particles with high surface activity can directly react with dye molecules, leading to the decolorization of dye. The reaction between Fe^0 and H_2O or H^+ can generate atom H, which induce the cleavage of azo bond (–N=N–), thus destroying the chromophore group and conjugated system of the azo dye. Moreover, the intermediate products of Fe^0 such as Fe^{2+}, Fe^{3+}, $Fe(OH)y^{2-y}$ and $Fe(OH)x^{3-x}$ were thermodynamically unstable and active [22]. During the reaction, iron corrosion and H^+ consumption lead to the increase of solution pH (final pH is 8–9). The formed passive iron oxides layers (Fe_3O_4, Fe_2O_3, $Fe(OH)_3$, and FeOOH) [27–29] could also adsorb dye molecules via the sulfonic group and reduce the colority of the dye wastewater through the formation of a bridged bidentate complex [30].

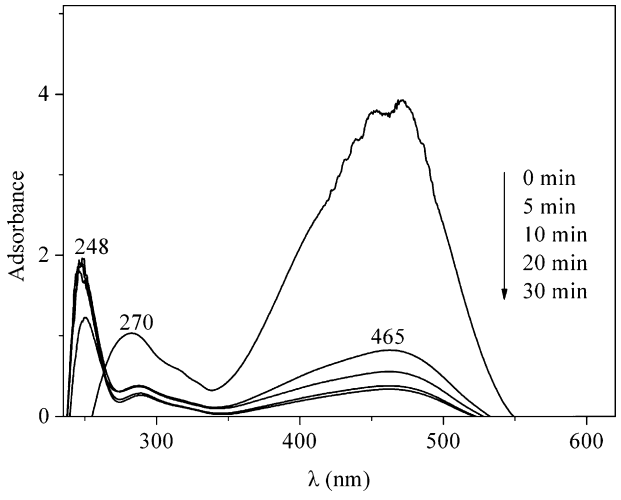

Fig. 3. UV–vis spectra of MO during the decolorization process: initial MO concentration, 50 mg/L; NZVI dosage, 0.3 g/L; initial pH 6; t = 30 °C.

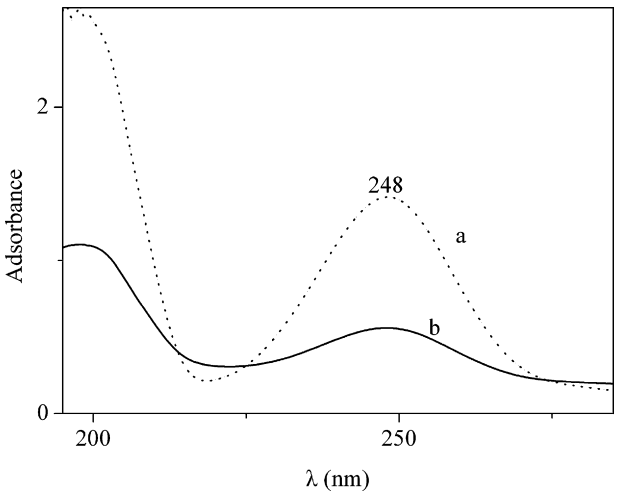

Fig. 4. UV–vis spectra of standard solution of sulfanilic acid (a) and the decolorized solution (b).

Fig. 3 illustrates the typical UV–vis spectra of MO during decolorization process. The strong absorbance band at 465 nm originates from a conjugated structure formed by the azo bond under the strong influence of the electron-donating dimethylamino group, and the band at 270 nm is ascribed to the $\pi \rightarrow \pi^*$ transition related to aromatic rings [31]. After 5 min reaction, the bands at 465 and 270 nm all became weaker, but the new band at 248 nm appeared. In summary, the spectra revealed the cleavage of the azo bond and the formation of the products. The band at 248 nm was possibly ascribed to sulfanilic acid, as compared with UV–vis spectra of the standard solution of sulfanilic acid (shown in Fig. 4). Therefore, we speculated that sulfanilic acid is one of the products. The other products were further analyzed by using GC–MS. Their GC retention times (t_R), molecular weights (M_W) and main fragments are summarized in Table 1. The sample shows two m/z peaks at 136 and 122, and they attributed to N, N-dimethyl-p-phenylenediamine and N-methyl-p-phenylenediamine, respectively.

3.3. Effects of initial MO concentration and reaction time

Series of experiments were carried out to study the effects of initial MO concentration and reaction time on the decolorization efficiency. As shown in Fig. 5, at a given experimental condition, decolorization time increased as the initial MO concentration increased. In general, the reaction proceeded rapidly within the first 10 min, and then slowed down. The possible reason is that at the early stage, dye molecules could easily transport to Fe^0 surface because of the strong adsorption and reduction ability of NZVI. Moreover, the bubbling of the generated H_2 in the system may cause the convection of the water and particles, and prevent the particles accumulation, remove the alteration products from particles, thus keeping the fresh surfaces and high reactivity of the particles [32]. As the reaction continued, solution pH increased, H_2 gas released became less, the convection of the water and particles was markedly reduced, the surface reactivity sites of Fe^0 particles were gradually occupied by corrosion products, and the MO concentration decreased. These factors would decrease the reaction rate greatly.

3.4. Effect of the NZVI dosage

To evaluate the effect of the NZVI dosage on the decolorization efficiency, MO concentration was fixed at 100 mg/L. In the reaction process, the variation of MO concentration with differ-

Table 1
Results of GC-MS analysis.

products	t_R (min)	M_W	Main fragment ions (m/z)
N,N-dimethyl-p-phenylenediamine	10.39	136	136,121,105,93,77,65,51,42
N-methyl-p-phenylenediamine	13.16	122	122,105,77,51

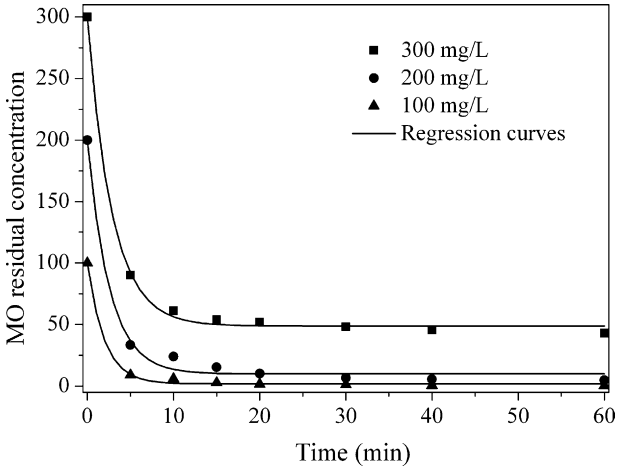

Fig. 5. Effect of the initial MO concentrations on decolorization efficiency of MO: NZVI dosage, 0.5 g/L; initial pH 6, t = 30 °C.

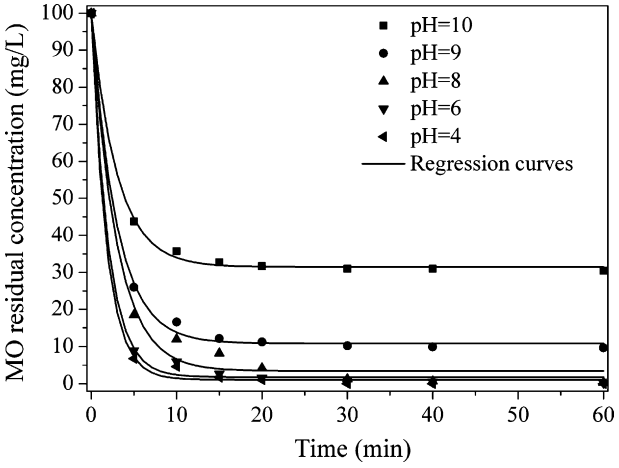

Fig. 7. Effect of solution pH on the decolorization efficiency of MO: initial MO concentration, 100 mg/L; NZVI dosage, 0.5 g/L; t = 30 °C.

ent NZVI dosages was shown in Fig. 6. As the reaction occurred at the Fe^0–H_2O interface, the more the NZVI loading, more is the iron surface area and the adsorptive and active sites. It can be seen from Fig. 6 that at the same reaction time, higher decolorization efficiency was obtained under higher NZVI loading. For example, within 60 min reaction, the decolorization efficiency was found to be 70.3%, 90.6%, 97.1% and 100%, respectively, for the NZVI dosages of 0.2, 0.3, 0.4, 0.5 g/L. However, it is not necessary to use a much higher iron dosage because the difference in the decolorization efficiency was rather small as the iron dosage increased to a certain degree.

3.5. Effect of initial pH

Solution pH has been considered as one of the important factors in Fe^0-contaminant systems. The results by Yang and Lee [21] showed that the degradation of nitrate by NZVI was an acid-driven process. For the most of the dye wastewater, their pH was in the range of 6–10. In this work, therefore, the effect of initial solution pH on the decolorization of MO by NZVI was studied in a pH range of 4–10, and the results were shown in Fig. 7. It was found that during the first period of reaction (10 min), initial pH had a significant effect on the decolorization efficiency. Nevertheless, this effect diminished with the longer reaction times. At the initial pH 4, 6, 8, MO solutions were almost completely decolorized within 60 min reaction. As the initial pH increased up to 10, the final decolorization efficiency decreased to 69.5% in the same reaction time. This can be ascribed to the fact that at the lower pH (<pHpzc ≈ 8, pzc stands for the point of zero charge), the surface of iron is positively charged [28], and the dyes molecules with a sulfuric group were negatively charged, which is favorable for the adsorption of dye onto the iron surface. When the solution pH is above the isoelectric point, the oxide surface becomes negatively charged, and Fe^0 surface could be easily covered by the corrosion products in alkaline conditions. However, even at the initial pH 9, more than 90% decolorization efficiency can be obtained within 60 min. This result

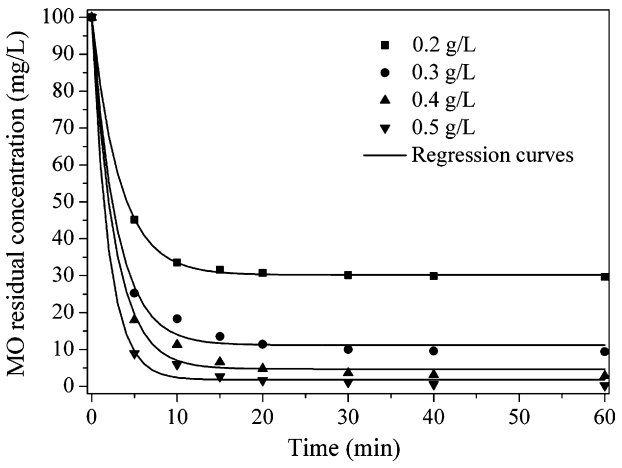

Fig. 6. Effect of NZVI dosage on the decolorization efficiency of MO: initial MO concentration, 100 mg/L; initial pH 6; t = 30 °C.

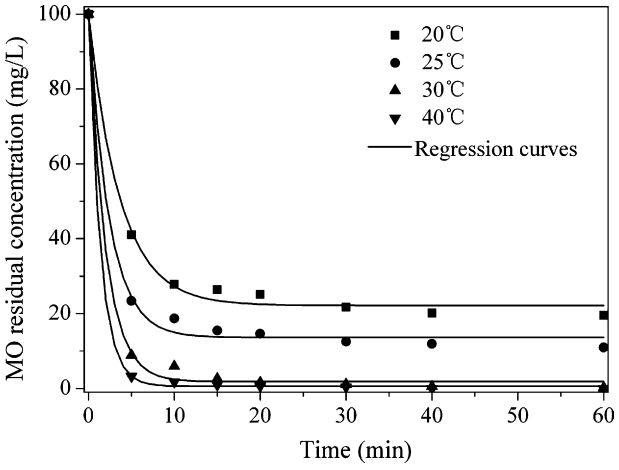

Fig. 8. Effect of temperature on the decolorization efficiency of MO: initial MO concentration, 100 mg/L; NZVI dosage, 0.5 g/L; initial pH 6.

suggests that weak acidic and circum-neutral initial pH favored dye decolorization, but the reaction may be retarded in the alkaline pH range. In general, this finding has a very practical meaning because it is not necessary to add any acid into the reaction system continuously or to use a buffer solution in the reaction process in order to hold the reaction system at acidic condition.

3.6. Effect of reaction temperature

Usually, chemical reaction is very sensitive to the changes of temperature, and temperature effect is important in providing some insight into the reaction mechanism [27]. In the present work, experiments were carried out in a temperature range of 20–40 °C to study the temperature effect on the decolorization of MO. As shown in Fig. 8, lower temperatures caused incomplete decolorization of MO within 60 min, and raising the temperature has a positive impact on the decolorization. The decolorization efficiency within 10 min reaction increased from 72.2% to 98.3% as the result of the temperature increase from 20 to 40 °C. It is obviously proved that higher reaction temperature can reduce the time required for MO decolorization. Since temperature of the discharged dye wastewater is usually higher, it is just convenient for the application of this technology.

3.7. Effect of sodium sulfate

The composition of the real dye wastewater is always complex. The dyeing wastewater includes lots of inorganic salts such as Na_2SO_4, which is a commonly used promoter and buffering agent in dyeing industry. So the effect of Na_2SO_4 was also studied in this work, and the results were shown in Fig. 9. It can be seen that Na_2SO_4 had a negative effect on the decolorization of MO by NZVI. The decolorization efficiency within 60 min reaction decreased from 100% to 84.6% as the concentration of Na_2SO_4 increased from 0 to 2.0 g/L. It is said that salt with higher concentration could lead to the increase in aggregation tendency of dye molecules [33]. To test the effect of salt on the aggregation of dye molecules, the UV–vis characterization experiment was carried out with Na_2SO_4 concentration in a range of 0–20 g/L. The obtained results were shown in Fig. 10. The UV–vis spectra of MO solution in the presence of different concentration of Na_2SO_4 were overlapped, which means that the effect of salt was not clearly on the aggregation of dye molecules in the research range. Therefore, the possible reason for the decrease of the decolorization efficiency caused by Na_2SO_4 is that, NZVI particles have an outside iron oxide surface

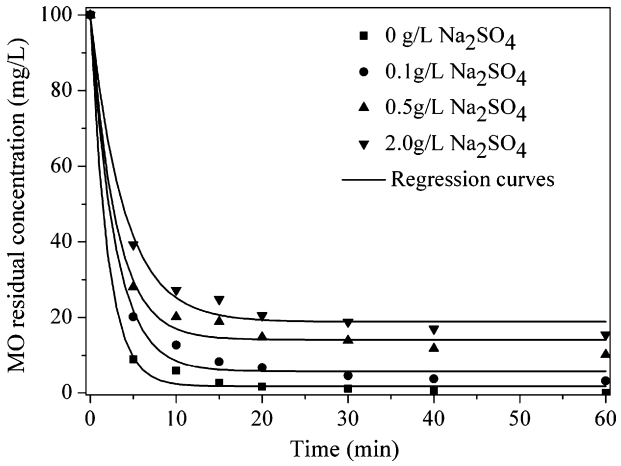

Fig. 9. Effect of sodium sulfate on the decolorization efficiency of MO: initial MO concentration, 100 mg/L; NZVI dosage, 0.5 g/L; initial pH 6, t = 30 °C.

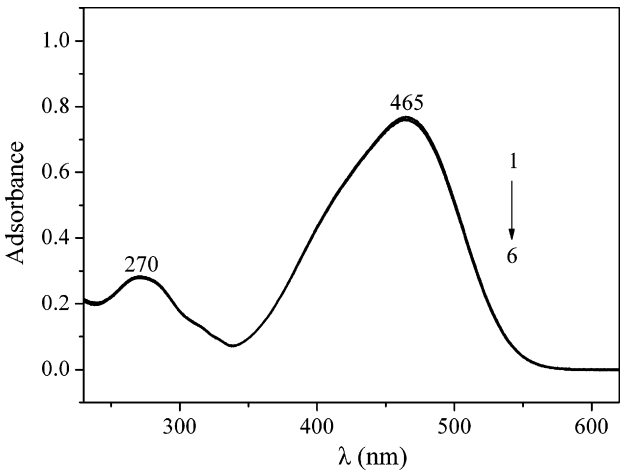

Fig. 10. UV–vis spectra of MO solution in the presence of Na_2SO_4 MO concentration, 10 mg/L; Na_2SO_4 concentration, (1) 0, (2) 0.05, (3) 0.2, (4) 1.0, (5) 5.0, (6) 20 g/L.

which is positively charged under the isoelectric point, and anions that have atoms with a lone pair of electrons can be adsorbed onto the surface of the particles through a coordinate bond, so SO_4^{2-} anions could compete with MO in occupying the adsorptive and reactive sites of the NZVI particle surfaces because they have the similar anion structure, thus leading to the decrease of the decolorization efficiency.

3.8. Kinetics analysis

Literature survey [22,23,27,34] reveals that in the NZVI-contaminant systems, kinetics patterns were generally treated as first or pseudo-first-order model with respect to contaminant concentration. However, Yang and Lee [21] and Wang et al. [35] reported that the degradation of nitrate by NZVI did not comply with first order kinetics. It is known that the reaction in ZVI-contaminant systems is a surface-mediated process. Thus the reaction rates are not only related to the contaminant concentration, but also related to the active surface sites of Fe^0. If the active surface of Fe^0 was regarded as invariable, the reaction could be treated as pseudo-first-order kinetics. However, once the active sites have been saturated, the transfer at contaminant and Fe^0 particle interface may be limited by mass transfer [36]. The reaction may deviate from first order kinetics because the decaying of surface activity during the reaction process. In addition, the pseudo-first-order model is always based on a single site type, and does not account for the effect of contaminants adsorption to non-reactive sites on the iron surface [37].

According to our experimental dada, the residual MO concentration can be expressed by the empirical equation

$$C_t = C_{\text{ultimate}} + (C_0 - C_{\text{ultimate}}) \times \alpha \times \exp(-kt) \quad (3)$$

proposed by Shu et al. [24]. Where C_0 is the initial MO concentration, C_t is the residual MO concentration at reaction time t, C_{ultimate} is the ultimate residual MO concentration, α represents the variation coefficient for each test and k denotes the empirical rate constant (min^{-1}). The constants C_{ultimate}, α, and k were obtained by nonlinear regression (first order exponential decay) from the experimental data. The results are given in Table 2. It can be seen that α value are all close to 1, so Eq. (3) can be changed into the equation,

$$C_t = C_{\text{ultimate}} + (C_0 - C_{\text{ultimate}}) \times \exp(-kt) \quad (4)$$

The correlation coefficients (r^2) indicated that the decolorization process fits well with first order exponential decay kinetics.

Table 2
Results of nonlinear regression of the experimental data.

C_0 (mg/L)	NZVI dosage (g/L)	Initial pH	t (°C)	C_{Na2SO4} (g/L)	$C_{ultimate}$ (mg/L)	α	k (min^{-1})	r^2
100	0.5	6	30	0	1.8114	0.9998	0.511	0.9978
200	0.5	6	30	0	9.8528	0.9988	0.392	0.9936
300	0.5	6	30	0	48.8222	0.9992	0.351	0.9982
100	0.2	6	30	0	30.0277	0.9997	0.306	0.9998
100	0.3	6	30	0	11.2130	0.9982	0.346	0.9951
100	0.4	6	30	0	4.7167	0.9988	0.372	0.9961
100	0.5	4	30	0	1.1088	0.9999	0.559	0.9983
100	0.5	8	30	0	3.4456	0.9976	0.342	0.9906
100	0.5	9	30	0	10.8368	0.9988	0.339	0.9982
100	0.5	10	30	0	31.4636	0.9989	0.331	0.9985
100	0.5	6	20	0	22.1787	0.9978	0.272	0.9945
100	0.5	6	25	0	13.6125	0.9993	0.416	0.9953
100	0.5	6	40	0	0.3538	1	0.723	0.9998
100	0.5	6	30	0.1	5.7284	0.9984	0.354	0.9950
100	0.5	6	30	0.5	15	0.9972	0.339	0.9854
100	0.5	6	30	2.0	18.8482	0.9955	0.254	0.9922

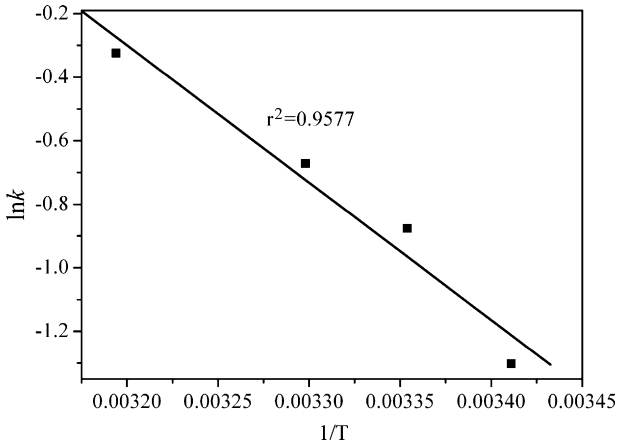

Fig. 11. Arrhenius plot of ln$k$ versus 1/T for the decolorization of MO by NZVI: initial MO concentration,100 mg/L; NZVI dosage, 0.5 g/L; initial pH 6; t = 30 °C.

Based on the obtained kinetic rate constants at different temperatures, the activation energy of the decolorization process of MO by NZVI can be obtained according to Arrhenius equation

$$\ln k = -\frac{Ea}{RT} + \ln A \quad (5)$$

The plots of ln$k$ versus 1/T were shown in Fig. 11. Obviously, good linear relationships have been observed between ln$k$ and 1/T. It was calculated that the activation energy Ea = 35.9 kJ/mol for the ecolorization process of MO by NZVI over the temperature range of 20–40 °C. Considering the fact that the activation energy for ordinary thermal reactions is usually between 60 and 250 kJ/mol [3], our result implied that the decolorization of MO aqueous solution by NZVI particles required a relatively low energy.

4. Conclusions

This work provided a potential technique for the pre-treatment of hardly degradable azo dye wastewater. Based on the discussion above, the following conclusions can be drawn:

(i) Decolorization of aqueous MO solution by NZVI particles was a rapid process, and can almost be completed in about 10 min. The main roles of the NZVI particles played in the decolorization process were adsorption, reduction and catalysis. The products identified by UV–vis characterization and GC–MS analysis were sulfanilic acid, N,N-dimethyl-p-phenylenediamine and N-methyl-p-phenylenediamine.

(ii) Kinetic studies suggest that the decolorization process can be described by the first order exponential decay kinetic model. The increase in temperature could greatly accelerate the decolorization. The activation energy Ea = 35.9 kJ/mol for the decolorization reaction under the experimental conditions.

(iii) An appropriate dosage of NZVI was important for the decolorization of MO. Generally, a greater iron dosage could yield greater reaction rate and decolorization efficiency. Under the same NZVI dosage, decolorization efficiency increase with the decrease of initial MO concentration.

(iv) The final decolorization efficiency at initial solution pH 4, 6, 8 was close to 100%, even at initial pH 9, the decolorization efficiency could achieve 90% within 60 min reaction. Therefore, no pH adjustment is needed for the treatment of azo dye wastewater.

(v) The existence of Na_2SO_4 could inhibit the decolorization of MO in some extent. The possible reason is that SO_4^{2-} ions could compete with MO in occupying the adsorptive and reactive sites of the NZVI particle surfaces.

Acknowledgements

The authors thank the Science and Technology Commission of Henan Province (no. 072102320007) and Henan Key Laboratory for Environmental Pollution Control for financial supports.

References

[1] H. Park, W. Choi, Visible light and Fe(III)-mediated degradation of acid Orange 7 in the absence of H_2O_2, J. Photochem. Photobiol. A Chem. 159 (2003) 241–247.
[2] K. Dutta, S. Mukhopadhyay, S. Bhattacharjee, B. Chaudhuri, Chemical oxidation of methylene blue using a Fenton-like reaction, J. Hazard. Mater. 84 (2001) 57–71.
[3] J. Chen, L. Zhu, Heterogeneous UV-Fenton catalytic degradation of dyestuff in water with hydroxyl-Fe pillared bentonite, Catal. Today 126 (2007) 463–470.
[4] R.R. Ozer, J.L. Ferry, Investigation of the photocatalytic activity of TiO_2-polyoxometalate systems, Environ. Sci. Technol. 35 (2001) 3242–3246.
[5] A.D. Bokare, R.C. Chikate, C.V. Rode, K.M. Paknikar, Iron-nickel bimetallic nanoparticles for reductive degradation of azo dye Orange G in aqueous solution, Appl. Catal. B: Environ. 79 (2008) 270–278.
[6] H. Liu, G. Li, J. Qu, H. Liu, Degradation of azo dye Acid Orange 7 in water by Fe^0/granular activated carbon system in the presence of ultrasound, J. Hazard. Mater. 144 (2007) 180–186.
[7] G. Mezohegyi, A. Kolodkin, U.I. Castro, C. Bengoa, F. Stuber, J. Font, A. Fabregat, A. Fortuny, Effective anaerobic decolorization of azo dye Acid Orange 7 in continuous upflow packed-bed reactor using biological activated carbon system, Ind. Eng. Chem. Res. 46 (2007) 6788–6792.
[8] J.P. Saxe, B.L. Lubenow, P.C. Chiu, C.P. Huang, D.K. Cha, Enhanced biodegradation of azo dyes using an integrated elemental iron-activated sludge system: I, Evaluation of system performance, Water Environ. Res. 78 (2006) 19–25.
[9] S. Nam, P.G. Tratnyek, Reduction of azo dyes with zero-valent iron, Water Res. 34 (2000) 1837–1845.

[10] M. Hou, F. Li, X. Liu, X. Wang, H. Wan, The effect of substituent groups on the reductive degradation of azo dyes by zerovalent iron, J. Hazard. Mater. 145 (2007) 305–314.
[11] M.C. Chang, H.Y. Shu, H.H. Yu, Y.C. Sung, Reductive decolourization and total organic carbon reduction of the diazo dye CI Acid Black 24 by zero-valent iron powder, J. Chem. Technol. Biotechnol. 81 (2006) 1259–1266.
[12] J.R. Perey, P.C. Chiu, C.P. Huang, D.K. Cha, Zero-valent iron pretreatment for enhancing the biodegradability of azo dyes, Water Environ. Res. 74 (2002) 221–225.
[13] J.T. Nurmi, P.G. Tratnyek, V. Sarathy, D.R. Baer, J.E. Amonette, K. Pecher, C. Wang, J.C. Linehan, D.W. Matson, R.L. Penn, M.D. Driessen, Characterization and properties of metallic iron nanoparticles: spectroscopy, electrochemistry, and kinetics, Environ. Sci. Technol. 39 (2005) 1221–1230.
[14] Y. Liu, G.V. Lowry, Effect of particle age (Fe^0 Content) and solution pH on NZVI reactivity: H_2 evolution and TCE dechlorination, Environ. Sci. Technol. 40 (2006) 6085–6090.
[15] H. Song, E.R. Carraway, Catalytic hydrodechlorination of chlorinated ethenes by nanoscale zero-valent iron, Appl. Catal. B: Environ. 78 (2008) 53–60.
[16] V. Sarathy, P.G. Tratnyek, J.T. Nurmi, D.R. Baer, J.E. Amonette, C.L. Chun, R.L. Penn, E.J. Reardon, Aging of iron nanoparticles in aqueous solution: effects on structure and reactivity, J. Phys. Chem. C 112 (2008) 2286–2293.
[17] T.T. Lim, J. Feng, B.W. Zhu, Kinetic and mechanistic examinations of reductive transformation pathways of brominated methanes with nano-scale Fe and Ni/Fe particles, Water Res. 41 (2007) 875–883.
[18] B.A. Manning, J.R. Kiser, H. Kwon, S.R. Kanel, Spectroscopic investigation of Cr(III)- and Cr(VI)-treated nanoscale zerovalent iron, Environ. Sci. Technol. 41 (2007) 586–592.
[19] A.B.M. Giasuddin, S.R. Kanel, H. Choi, Adsorption of humic acid onto nanoscale zerovalent iron and its effect on arsenic removal, Environ. Sci. Technol. 41 (2007) 2022–2027.
[20] O. Çelebi, Ç. Üzüm, T. Shahwan, H.N. Erten, A radiotracer study of the adsorption behavior of aqueous Ba^{2+} ions on nanoparticles of zero-valent iron, J. Hazard. Mater. 148 (2007) 761–767.
[21] G.C.C. Yang, H.L. Lee, Chemical reduction of nitrate by nanosized iron: kinetics and pathways, Water Res. 39 (2005) 884–894.
[22] K. Sohn, S.W. Kang, S. Ahn, M. Woo, S.K. Yang, Fe(0) nanoparticles for nitrate reduction: stability, reactivity, and transformation, Environ. Sci. Technol. 40 (2006) 5514–5519.
[23] Z. Xiong, D. Zhao, G. Pan, Rapid and complete destruction of perchlorate in water and ion-exchange brine using stabilized zero-valent iron nanoparticles, Water Res. 41 (2007) 3497–3505.
[24] H.Y. Shu, M.C. Chang, H.H. Yu, W.H. Chen, Reduction of an azo dye Acid Black 24 solution using synthesized nanoscale zerovalent iron particles, J. Colloid Interface Sci. 314 (2007) 89–97.
[25] G.N. Glavee, K.J. Klabunde, C.M. Sorensen, G.C. Hadjipanayis, Chemistry of borohydride reduction of iron(II) and iron(III) ions in aqueous and nonaqueous media. Formation of nanoscale Fe, FeB, and Fe_2B powders, Inorg. Chem. 34 (1995) 28–35.
[26] Y.P. Sun, X. Li, J. Cao, W. Zhang, H.P. Wang, Characterization of zero-valent iron nanoparticles, Adv. Colloid Interface Sci. 120 (2006) 47–56.
[27] Y.H. Liou, S.L. Lo, C.J. Lin, W.H. Kuan, S.C. Weng, Chemical reduction of an unbuffered nitrate solution using catalyzed and uncatalyzed nanoscale iron particles, J. Hazard. Mater. 127 (2005) 102–110.
[28] X. Li, D.W. Elliott, W. Zhang, Zero-valent iron nanoparticles for abatement of environmental pollutants: materials and engineering aspects, Crit. Rev. Solid State Mater. Sci. 31 (2006) 111–122.
[29] J.A. Mielczarski, G.M. Atenas, E. Mielczarski, Role of iron surface oxidation layers in decomposition of azo-dye water pollutants in weak acidic solutions, Appl. Catal. B: Environ. 56 (2005) 289–303.
[30] J. Bandara, J.A. Mielczarski, J. Kiwi, 1.Molecular mechanism of surface recognition. Azo dyes degradation on Fe, Ti, and Al oxides through metal sulfonate complexes, Langmuir 15 (1999) 7670–7679.
[31] C. Galindo, P. Jacques, A. Kalt, Photodegradation of the aminoazobenzene acid orange 52 by three advanced oxidation processes: UV/H_2O_2, UV/TiO_2 and VIS/TiO_2: comparative mechanistic and kinetic investigations, J. Photochem. Photobiol. A: Chem. 130 (2000) 35–47.
[32] E.J. Reardon, R. Fagan, J.L. Vogan, A. Przepiora, Anaerobic corrosion reaction kinetics of nanosized iron, Environ. Sci. Technol. 42 (2008) 2420–2425.
[33] Y. Dong, J. Chen, C. Li, H. Zhu, Decoloration of three azo dyes in water by photocatalysis of Fe(III)eoxalate complexes/H_2O_2 in the presence of inorganic salts, Dyes Pigments 73 (2007) 261–268.
[34] H. Song, E.R. Carraway, Reduction of chlorinated ethanes by nanosized zero-valent iron: kinetics, pathways, and effects of reaction conditions, Environ. Sci. Technol. 39 (2005) 6237–6245.
[35] W. Wang, Z. Jin, T. Li, H. Zhang, S. Gao, Preparation of spherical iron nanoclusters in ethanol-water solution for nitrate removal, Chemosphere 65 (2006) 1396–1404.
[36] S.M. Ponder, J.G. Darab, T.E. Mallouk, Remediation of Cr(VI) and Pb(II) aqueous solutions using supported, nanoscale zero-valent iron, Environ. Sci. Technol. 34 (2000) 2564–2569.
[37] R. Venkatapathy, D.G. Bessingpas, S. Canonica, J.A. Perlinger, Kinetics models for trichloroethylene transformation by zero-valent iron, Appl. Catal. B: Environ. 37 (2002) 139–159.